since it is expected to be a dominant quenching pathway in donor media. This effect is intriguing because, in the case of $Cu(dmp)_2^+$, exciplex quenching proceeds with a negative activation energy due to the bond making that attends exciplex formation.[15] In other words, the quenching is *less* efficient at higher temperature. The data in Figure 4 clearly require that the activation energy for solvent-induced quenching be positive. The difference in the activation requirement can be understood in terms of the ligand–ligand repulsion forces that come into play when the already crowded coordination sphere of $Cu(dmp)(PPh_3)_2^+$ has to expand to accept another ligand. Unfortunately, we have been unable to measure activation barriers for $Cu(dmp)(PPh_3)_2^+$ directly. Although various Lewis bases quench the emission, they also compete with PPh_3 for coordination to the copper center in the ground state, confusing speciation.

The temperature dependence of the emission from $Cu(phen)(PPh_3)_2^+$ in methanol does, however, provide additional support for the above interpretation. The fact that the luminescence intensity of $Cu(phen)(PPh_3)_2^+$ is nearly independent of temperature in methanol suggests that the barrier to quenching is significantly smaller in this case, although still positive. According to our model, a smaller barrier would be expected because the steric forces are reduced in the less crowded phen complex.[9]

Conclusions

The speciation of mixed-ligand copper(I) systems is found to be sensitive to steric and electronic effects associated with the ligands as well as the nature of the counterion and the dielectric constant of the solvent. Conditions have been found such that the absorption and the emission spectra of $Cu(dmp)(PPh_3)_2^+$ and $Cu(phen)(PPh_3)_2^+$ can be studied in solution. In methanol, $Cu(dmp)(PPh_3)_2^+$ is a relatively strong emitter because steric crowding inhibits solvent-induced exciplex quenching. Under these circumstances exciplex quenching is a thermally activated process, which dominates the temperature dependence of the emission yield. A lower barrier to quenching occurs in the less crowded $Cu(phen)(PPh_3)_2^+$ complex. As a result, the quantum yield of emission is sharply reduced and only weakly temperature-dependent in methanol. $Cu(phen)(PPh_3)_2^+$ can also be studied in the less nucleophilic solvent methylene chloride, wherein solvent-induced quenching is less of a problem. Under these conditions the luminescence intensity increases with increasing temperature, as it does in the solid state. This is explained by thermal population of a singlet CT state with a favorable radiative rate constant.

Acknowledgment. This work was supported by the National Science Foundation through Grant No. CHE-8414267. We also acknowledge Alan A. Del Paggio, who first measured the temperature dependence of the emission from $Cu(dmp)(PPh_3)_2^+$ in methanol, and Robert M. Berger, who assisted with some of the lifetime measurements.

Registry No. $Cu(dmp)(PPh_3)_2^+$, 78809-58-2; $Cu(phen)(PPh_3)_2^+$, 47886-23-7.

Contribution from the Institut für Anorganische Chemie und Analytische Chemie, Johannes-Gutenberg-Universität, 6500 Mainz, FRG

Investigation of the $^1A_1 \rightleftharpoons {}^5T_2$ Intersystem Crossing Dynamics of an Iron(II) Spin-Crossover Complex in the Solid State by Mössbauer Spectroscopy

P. Adler,† H. Spiering, and P. Gütlich*

Received February 25, 1987

A very gradual thermal high-spin (HS) ⇌ low-spin (LS) transition of the ferrous ion in $[Fe(2\text{-pic})_3](PF_6)_2$ (2-pic = 2-(aminomethyl)pyridine) has been observed by Mössbauer and susceptibility measurements. Above 200 K the $^1A_1 \rightleftharpoons {}^5T_2$ intersystem crossing rates are comparable to the hyperfine frequencies leading to typical Mössbauer relaxation spectra. The rate constants are derived from a line shape analysis employing the stochastic theory of line shape. Their temperature dependence is described by an Arrhenius equation with the activation energies ΔE_{LH} = 20.6 (6) kJ mol^{-1} and ΔE_{HL} = 12.5 (8) kJ mol^{-1} for the LS → HS and HS → LS conversions, respectively. The frequency factors are $A_{LH} \sim 3 \times 10^{11}$ s^{-1} and $A_{HL} \sim 1 \times 10^9$ s^{-1}. The activation parameters are compared with the existing liquid-solution data.

Introduction

Studies of various d^5 and d^6 spin-crossover complexes revealed that the temperature interval and the shape of the high-spin (HS) ⇌ low-spin (LS) transition curves in the solid state are determined to a large extent by the influence of the lattice.[1-3] Also, the question as to what extent the dynamics of the HS ⇌ LS equilibrium is affected by the lattice has found interest.[4,5] From the molecular point of view the HS ⇌ LS conversion is an intersystem crossing (ISC) with $\Delta S = 2$ for iron(II) complexes and iron(III) complexes, and $\Delta S = 1$ for Co(II) complexes. Therefore, the study of the dynamics of the HS ⇌ LS equilibrium may be useful to gain a deeper insight in the factors governing ISC processes that occur in photophysics, photochemistry, and also in some electron-transfer reactions of biological systems. The dynamical nature of the spin equilibrium has been well established for iron(II), iron(III), and cobalt(II) complexes in solution by using different techniques[6-14] and for a number of solid iron(III) complexes with Mössbauer spectroscopy.[4,5,15-21] Whereas quantitative data about the ISC rates and their temperature dependence are available for a variety of complexes in solution,[6-14] such data are rather scarce for the solid state. The order of magnitude of the ISC rates k in the solid state can be estimated from the line shape of the Mössbauer spectra. If k is small, relative to the hyperfine fre-

† In partial fulfillment of the Ph.D. thesis.

(1) König, E.; Ritter, G.; Kulshreshta, S. K. *Chem. Rev.* **1985**, *85*, 219.
(2) (a)Gütlich, P *Struct. Bonding (Berlin)* **1981**, *44*. (b) Gütlich, P. In *Chemical Mössbauer Spectroscopy*; Herber, R. H., Ed.; Plenum: New York, 1984; pp 27-64.
(3) Haddad, M. S.; Lynch, M. W.; Federer, W. D.; Hendrickson, D. N. *Inorg. Chem.* **1981**, *20*, 123.
(4) (a) Timken, M. D.; Strouse, C. E.; Soltis, S. M.; Daverio, S.; Hendrickson, D. N.; Abdel-Mawgoud, A. M.; Wilson, S. R. *J. Am. Chem. Soc.* **1986**, *108*, 395. (b) Timken, M. D.; Abdel-Mawgoud, A. M.; Hendrickson, D. N. *Inorg. Chem.* **1986**, *25*, 160.
(5) (a) Maeda, Y.; Tsutsumi, N.; Takashima, Y. *Inorg. Chem.* **1984**, *23*, 2440. (b) Maeda, Y.; Oshio, H.; Takashima, Y.; Mikuriya, M.; Hidaka, M. *Inorg. Chem.* **1986**, *25*, 2958.
(6) Hoselton, M. A.; Drago, R. S.; Wilson, L. J.; Sutin, N. *J. Am. Chem. Soc.* **1976**, *98*, 6967.
(7) Dose, E. V.; Hoselton, M. A.; Sutin, N.; Tweedle, M. F.; Wilson, L. J. *J. Am. Chem. Soc.* **1978**, *100*, 1141.
(8) Beattie, J. K.; Binstead, R. A.; West, R. J. *J. Am. Chem. Soc.* **1978**, *100*, 3044.
(9) Binstead, R. J.; Beattie, J. K.; Dose, E. W.; Tweedle, M. F.; Wilson, L. J. *J. Am. Chem. Soc.* **1978**, *100*, 5609.
(10) Binstead, R. A.; Beattie, J. K.; Dewey, T. G.; Turner, D. H. *J. Am. Chem. Soc.* **1980**, *102*, 6442.
(11) McGarvey, J. J.; Lawthers, I. *J. Chem. Soc., Chem. Commun.* **1982**, 906.
(12) Lawthers, I.; McGarvey, J. J. *J. Am. Chem. Soc.* **1984**, *106*, 4280.

0020-1669/87/1326-3840$01.50/0

quencies ω_{hf}, sharp distinct resonances for the different states are observed. On the other hand, averaged spectra with intermediate isomer shifts and quadrupole splittings are found for $k \gg \omega_{hf}$. If k and ω_{hf} are of comparable magnitude, broadened and asymmetric resonances are observed. In the latter case a quantitative line shape analysis reveals the rate constants from the Mössbauer spectra. The first examples of spin-crossover complexes that were found to interconvert rapidly within the Mössbauer time scale were some iron(III) dithiocarbamates.[15,16] Meanwhile, other iron(III) complexes with averaged Mössbauer spectra were also examined, revealing the dynamic nature of the spin equilibrium.[4,5,19,20] Maeda et al. attempted to evaluate such spectra with a two-state-relaxation model.[5,21] These evaluations are, however, unfavorable in the case of iron(III) complexes due to the presence of paramagnetic relaxation within the spin states. Paramagnetic relaxation itself gives rise to line broadening and asymmetries in the spectra,[22] which cannot be separated from relaxation between the spin states.

In contrast to ferric compounds nearly all ferrous spin-crossover complexes, that have been investigated so far show distinct resonances for the HS and the LS state. One exception is $[Fe(phen)_2(NCBH_3)_2]$, which exhibits a gradual HS $\rightleftharpoons$ LS transition above 300 K. The spectra of this compound were interpreted qualitatively by a three-state-relaxation model that assumes an additional intermediate spin state.[23] Line-broadening effects observed in ground samples of $[Fe(phen)_2(NCS)_2]$ have also been explained as spin-state-relaxation effects employing a two-state-relaxation model.[24]

In the present paper we report on the spin-crossover behavior of the polycrystalline complex $[Fe(2\text{-pic})_3](PF_6)_2$. We will demonstrate that the Mössbauer spectra above 200 K clearly reveal the dynamic nature of the spin equilibrium for this iron(II) complex. From a quantitative line shape analysis, the rate constants are determined as a function of temperature. These values will be compared with the results of the solution studies.

In addition, we performed a temperature-dependent susceptibility study in order to characterize the spin-transition curve independently of the Mössbauer spectra.

Experimental Section

Materials. The complex $[Fe(2\text{-pic})_3](PF_6)_2$ was prepared as described by Chum et al.[25] but with $FeCl_2 \cdot 2H_2O$ instead of $FeSO_4 \cdot 7H_2O$ as starting material. The zinc complex was prepared in an analogous way with $ZnCl_2$ as the metal salt component. The crude products were recrystallized from methanol. The purity of the compounds was checked by elemental analysis.

Susceptibility Measurements. The magnetic susceptibilities $\chi(T)$ for $[Fe(2\text{-pic})_3](PF_6)_2$ between 40 and 320 K were measured with a Foner type magnetometer, equipped with a helium flow cryostat, in an external field of 1 T. The diamagnetic correction for the ferrous complex was determined from a measurement of χ at room temperature for the diamagnetic zinc complex ($\chi = -385 \times 10^{-6}$ cm^3 mol^{-1}).

Mössbauer Spectroscopy. Mössbauer spectra of $[Fe(2\text{-pic})_3](PF_6)_2$ between 80 and 290 K have been recorded with a conventional Mössbauer spectrometer operating in the constant acceleration mode and equipped with a $^{57}Co/Rh$ source at room temperature. The sample was placed in an Oxford bath cryostat.

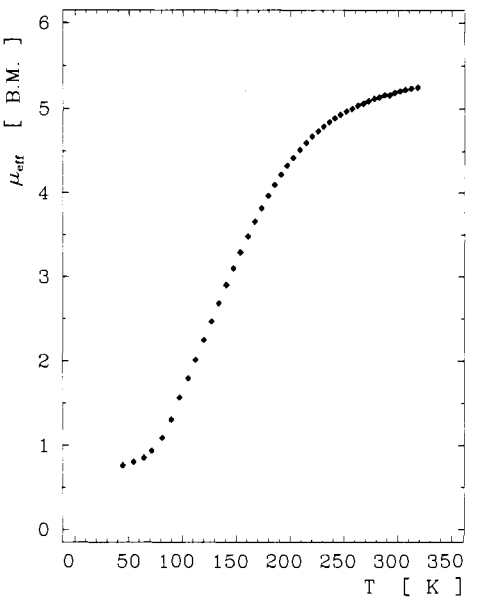

Figure 1. Effective magnetic moment μ_{eff} vs temperature T for $[Fe(2\text{-pic})_3](PF_6)_2$.

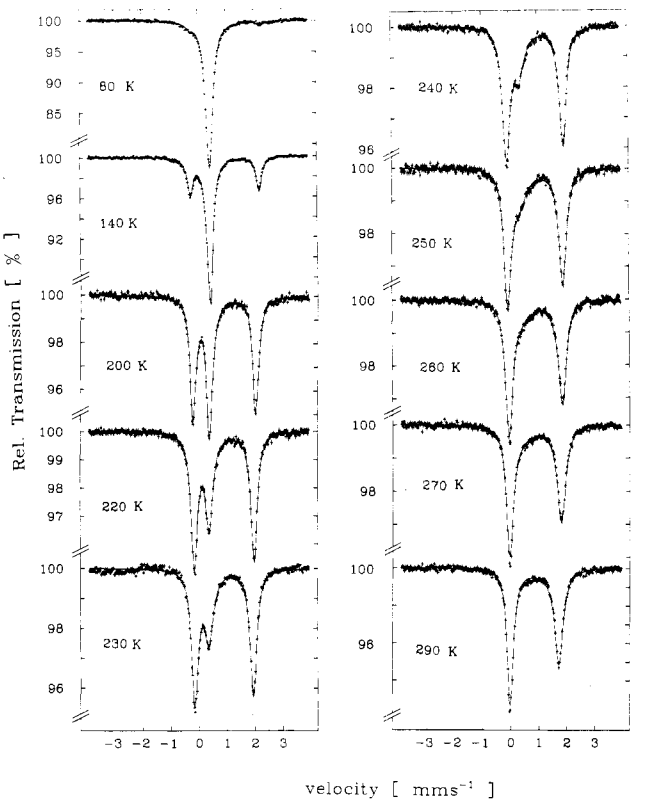

Figure 2. ^{57}Fe Mössbauer spectra of $[Fe(2\text{-pic})_3](PF_6)_2$. The solid lines are the best fits calculated with the two-state-relaxation model described in the text.

Results

Characterization of the Spin Transition in $[Fe(2\text{-pic})_3](PF_6)_2$. The plot of the effective magnetic moment μ_{eff} vs. temperature T (Figure 1) of $[Fe(2\text{-pic})_3](PF_6)_2$ shows a very gradual HS $\rightleftharpoons$ LS transition over the whole temperature range under study. Even above 300 K the spin transition is not yet complete. These results are confirmed by the Mössbauer spectra (Figure 2). At 80 K mainly an intense singlet with an isomer shift characteristic for LS iron(II) is found. The intensity of the quadrupole split doublet

(13) McGarvey, J. J.; Lawthers, I.; Heremans, K.; Toftlund, H. *J. Chem. Soc., Chem. Commun.* **1984**, 1575.
(14) DiBenedetto, J.; Arkle, V.; Goodwin, H. A.; Ford, P. C. *Inorg. Chem.* **1985**, *24*, 456.
(15) Merrithew, P. B.; Rasmussen, P. G. *Inorg. Chem.* **1972**, *11*, 325.
(16) Kunze, K. R.; Perry, D. L.; Wilson, L. J. *Inorg. Chem.* **1977**, *16*, 594.
(17) DeFilipo, D.; Dapalano, P.; Diaz, A.; Steffe, S.; Trogu, E. F. *J. Chem. Soc., Dalton Trans.* **1977**, 1566.
(18) Oshio, H.; Maeda, Y.; Takashima, Y. *Inorg. Chem.* **1983**, *22*, 2684.
(19) Federer, W. D.; Hendrickson, D. N. *Inorg. Chem.* **1984**, *23*, 3861.
(20) Federer, W. D.; Hendrickson, D. N. *Inorg. Chem.* **1984**, *23*, 3870.
(21) Maeda, Y.; Takashima, Y.; Matsumoto, N.; Ohyoshi, A. *J. Chem. Soc., Dalton Trans.* **1986**, 1115.
(22) Blume, M. *Phys. Rev. Lett.* **1965**, *14*, 96.
(23) Edwards, M. P.; Hoff, C. P.; Curnutts, B.; Eck, J. S.; Purcell, K. F. *Inorg. Chem.* **1984**, *23*, 2613.
(24) Gütlich, P.; Köhler, C. P.; Köppen, H.; Meissner, E.; Müller, E. W.; Spiering, H. *Proceedings of the International Conference on the Applications of the Mössbauer Effect*; Jaipur, India, 1981; Indian National Science Academy: New Delhi, India, 1982.
(25) Chum, H. L.; Vanin, J. A.; Holanda, M. J. D. *Inorg. Chem.* **1982**, *21*, 1146.

corresponding to the HS state is small. Surprisingly the LS resonance consists of a sharp single line in contrast with the Mössbauer spectra of the related complexes $[Fe(2\text{-pic})_3]Cl_2 \cdot (MeOH, EtOH)$ and $[Fe(2\text{-pic})_3]Br_2 \cdot EtOH$, which show also a quadrupole splitting in the LS state.[26-28]

Between 100 and 200 K the area fraction of the HS doublet increases, reflecting the LS → HS conversion. The resonances in this temperature interval are still sharp. Above 200 K the LS resonance line and, to a lesser extent, also the HS resonance lines broaden. Above 250 K only one asymmetric doublet is found. These features are characteristic for Mössbauer relaxation spectra, indicating that k becomes comparable with the hyperfine frequencies.

Stochastic Model for the HS ⇌ LS Relaxation. In order to obtain the ISC rates as a function of temperature, the spectra were evaluated with a two-state-relaxation model. The stochastic theory of Mössbauer lineshapes[29-31] has been used to describe a variety of dynamic phenomena in Mössbauer spectra. A recent description of the theory and its applications was given by Dattagupta;[32] its application to problems in inorganic chemistry was discussed by Hoy.[33] According to the theory the Mössbauer nucleus is governed by a time-dependent Hamiltonian fluctuating at random between a finite number of forms $\hat{H}_j$. The line shapes of Mössbauer spectra arising from this model were generally derived by Blume without further specifications of $\hat{H}_j$.[31] We start with his result for the cross section $\sigma(\omega)$ for the absorption process

$$\sigma(\omega) \sim \mathrm{Re}\,[\sum_{\substack{e,g\\ e',g'}} \langle e|\hat{V}^-|g\rangle^* \langle e'|\hat{V}^-|g'\rangle\, G_{ge,g'e'}(\mathrm{p})] \qquad (1)$$

with

$$G_{ge,g'e'}(p) = \sum_{jj'} \gamma_j [p\mathbf{E} - \mathbf{W} - i\mathbf{H}^x]_{jge,j'g'e'} \qquad (2)$$

In (1) and (2) the operator $\hat{V}^-$ describes the absorption of a photon, $|e\rangle$ and $|g\rangle$ represent the basis functions of the four excited states ($I = {}^3/_2$; e, $e' = 1, 2, 3, 4$) and the two ground states ($I = {}^1/_2$; g, $g' = 1, 2$), respectively. The a priori probability to find the system in the state $|j\rangle$ generating the nuclear Hamiltonian $\hat{H}_j$ is γ_j, and p abbreviates $\Gamma/2 - i\hbar\omega$ with the natural line width Γ. The matrix $[p\mathbf{E} - \mathbf{W} - i\mathbf{H}^x]$ consists of the matrix elements of the so-called superoperators $\hat{E}$, $\hat{W}$, and $\hat{H}^x$. $\hat{E}$ is the unitary superoperator, $\hat{W}$ is the relaxation superoperator, and $\hat{H}^x$ is the Liouville operator describing the hyperfine interaction. Following Blume,[31] first the matrix $[p\mathbf{E} - \mathbf{W} - i\mathbf{H}^x]$ is constructed and subsequently inverted. Its elements are given by

$$[p\mathbf{E} - \mathbf{W} - i\mathbf{H}^x]_{jge,j'g'e'} = p\delta_{gg'}\delta_{ee'}\delta_{jj'} - k_{jj'}\delta_{gg'}\delta_{ee'} - i(H_j^{gg'}\delta_{ee'} - H_j^{e'e}\delta_{g'g})\delta_{jj'} \qquad (3)$$

Here $H_j^{gg'}$ and $H_j^{e'e}$ are the matrix elements of the hyperfine Hamiltonians for the ground and excited states of the nuclei, respectively, if the system is in the state $|j\rangle$. The transition probability between the states $|j\rangle$ and $|j'\rangle$ per unit time is denoted as $k_{jj'}$. If it is assumed that the fluctuations may be described as a stationary Markov process, one obtains $\sum_{j'} k_{jj'} = 0$. Thus in the present case of a two-state-relaxation model, describing the relaxation between the LS state (L) and the HS state (H) the diagonal elements of the relaxation matrix $\mathbf{W}$ are given by

$$k_{LL} = -k_{LH} \qquad k_{HH} = -k_{HL} \qquad (4)$$

The nondiagonal elements fulfill the requirement of detailed balance

$$\gamma_H k_{HL} = \gamma_L k_{LH} = (1 - \gamma_H) k_{LH} \qquad (5)$$

In general the above matrix is of the rank $(2I_g + 1)(2I_e + 1)2$ for a two-state model, i.e. 16 for ^{57}Fe. The problem considered in this paper, however, is much simpler as quadrupole interaction occurs only in the HS state. The Hamiltonian $\hat{H}$ of the $^5T_{2g}$ state is the sum of the isomer shift operator $\hat{H}_{is}$ and the quadrupole interaction operator $\hat{H}_Q$, which is expressed by angular momentum operators $\hat{I}^2$ $\hat{I}_z$, and $\hat{I}_\pm$ as

$$\hat{H}_Q = eQV_{zz}[3\hat{I}_z^2 - \hat{I}^2 + \eta(\hat{I}_+^2 + \hat{I}_-^2)/2]/[4I(2I-1)] \qquad (6)$$

Q is the quadrupole moment of the nucleus, V_{zz} is the z component of the efg tensor in the principal axes system, and η is the asymmetry parameter. The quantities V_{zz}^H and η_H for the HS state are thermal averages over the contributions from the substates of the $^5T_{2g}$ state. The relaxation within these substates is rapid. As the Hamiltonian for the $^1A_{1g}$ state is given by the isomer shift operator $\hat{H}_{is}$ only and as the operators $\hat{H}_{is}$ are already diagonal with respect to the nuclear states, the operators $\hat{H}_H$ and $\hat{H}_L$ for the HS and LS state commute in the present case: $[\hat{H}_H, \hat{H}_L] = 0$. For a system whose Hamiltonians commute at different times, which was originally treated by Kubo and Anderson,[34] the diagonalization of the hyperfine Hamiltonian and the stochastic averaging can be separated.[31] Thus it follows from (3) that only the 2×2 matrices

$$\mathbf{G}_{ge} = \begin{pmatrix} p + i\hbar\omega_L^{ge} + k_{LH} & -k_{LH} \\ -k_{HL} & p + i\hbar\omega_H^{ge} + k_{HL} \end{pmatrix} \qquad (7)$$

have to be inverted. If the isomer shifts are denoted as δ_j (j = H,L) and the quadrupole splitting of the HS state is denoted as ΔE_Q^H, the hyperfine energies are given by

$$\hbar\omega_L^{ge} = \delta_L$$
$$\hbar\omega_H^{ge} = \delta_H \pm \Delta E_Q^H \,\mathrm{sign}\,(V_{zz}^H) \qquad (8)$$

The energy shift $\pm\Delta E_Q^H$ sign (V_{zz}^H) to $\hbar\omega_H^{ge}$ arises from the diagonalization of the Hamiltonian (6) with a positive sign for the eigenstates $|e = 1,2\rangle$ and a negative sign for $|e = 3,4\rangle$. Thus only two different values for G_{ge} exist, which will be denoted as G_+ and G_-. Performing the inversion of (7) and the sum in (2), one obtains

$$G_{ge}(p) = [\gamma_H(p + i\hbar\omega_L^{ge} + k_{LH} + k_{HL}) + \gamma_L(p + i\hbar\omega_H^{ge} + k_{HL} + k_{LH})]/[(p + i\hbar\omega_H^{ge} + k_{HL})(p + i\hbar\omega_L^{ge} + k_{LH}) - k_{HL}k_{LH}] \qquad (9)$$

It has been shown[35] that the stochastic theory according to Kubo and Anderson is mathematically equivalent to the rate theory of Wickman.[36] Thus the real part of (9) required for the calculation of $\sigma(\omega)$ is equivalent to the Wickman formula,[36] which is widely used for the evaluation of Mössbauer relaxation spectra. Inserting (9) into (1) and introducing the values for the intensity matrix elements $|\langle e|\hat{V}^-|g\rangle|^2$ and the prefactors omitted in (1), one finally obtains

$$\sigma(\omega) = \Gamma\sigma_0(\mathrm{Re}\,(G_+ + G_-))/2 \qquad (10)$$

where σ_0 is the cross section at resonance.

A result similar to (9) was recently obtained by Maeda et al.[21] employing a stochastic model according to Blume and Tijon[29,30] for the HS ⇌ LS relaxation. These authors considered the relaxation between HS and LS states with axially symmetric efg's in the same principal axes system and with identical isomer shifts.

(26) Sorai, M.; Ensling, J.; Gütlich, P. *Chem. Phys.* **1976**, *18*, 199.
(27) Sorai, M.; Ensling, J.; Hasselbach, K. M.; Gütlich, P. *Chem. Phys.* **1977**, *20*, 197.
(28) Wiehl, L.; Kiel, G.; Köhler, C. P.; Spiering, H.; Gütlich, P. *Inorg. Chem.* **1986**, *25*, 1565.
(29) Blume, M.; Tijon, J. A. *Phys. Rev.* **1968**, *165*, 446.
(30) Tijon, J. A.; Blume, M. *Phys. Rev.* **1968**, *165*, 456.
(31) Blume, M. *Phys. Rev.* **1968**, *174*, 351.
(32) Dattagupta, S. In *Advances in Mössbauer Spectroscopy*; Thosar, B. V., Iyengar, P. K., Eds.; Elsevier: Amsterdam, Oxford, New York, 1983; p 586.
(33) Hoy, G. R. In *Mössbauer Spectroscopy Applied to Inorganic Chemistry*; Long, G. J., Ed.; Plenum: New York, London, 1984; p 195.
(34) (a) Kubo, R. *J. Phys. Soc. Jpn.* **1954**, *9*, 935. (b) Anderson, P. W. *J. Phys. Soc. Jpn.* **1954**, *9*, 316.
(35) Nowik, J. *Phys. Lett. A* **1967**, *24A*, 487.
(36) Wickman, H. H.; Klein, M. P.; Shirley, D. A. *Phys. Rev.* **1966**, *152*, 345.

This situation may be readily analyzed in the manner described in the present paper. If the principal axes systems of the HS and LS efg's are identical and furthermore if $\eta_H = \eta_L$ the Hamiltonians $\hat{H}_H$ and $\hat{H}_L$ still commute as $\hat{H}_Q{}^H$ and $\hat{H}_Q{}^L$ given by (6) commute. Then again (9) is valid with

$$\hbar\omega_L{}^{ge} = \delta_L \pm \Delta E_Q{}^L(\text{sign } (V_{zz}{}^L))/2$$

and the resulting Mössbauer relaxation spectra also depend on (sign $(V_{zz}{}^L)$)(sign $(V_{zz}{}^H)$). It is not necessary to assume equal isomer shifts δ_H and δ_L as in ref 21.

In general, however, in the case of two efg's with different principal axes systems and $\eta_H \neq \eta_L$, the hyperfine Hamiltonians $\hat{H}_H$ and $\hat{H}_L$ do not commute and the Mössbauer relaxation spectra also depend on the relative orientations of the principal axes systems and on the asymmetry parameters.

Calculation of the Mössbauer Spectra. A Mössbauer spectrum is generally given by[37]

$$N(v) = N(\infty)[1 - f_s N_c(\infty)\ (1 - T(v))/N(\infty)] \qquad (11)$$

$N(v)$ is the counting rate at the Doppler velocity v, $N(\infty)$ is the base line, $N_c(\infty)$ is the background-corrected base line, f_s is the Debye–Waller factor of the source, and

$$T(v) = \int_{-\infty}^{\infty} S(\omega - v)\ \exp(-t_{\text{eff}}\ A(\omega))\ d\omega \qquad (12)$$

the transmission integral with the effective absorber thickness t_{eff} and the normalized cross section $A(\omega) = \sigma(\omega)/\sigma_0$ for the absorption process. In order to account for line-broadening effects, which are due to line broadening of the source by aging (clustering) and due to instrumental factors, the source function $S(\omega)$ was described by a convolution integral of a Lorentzian function $L(\omega - \omega')$ and a Gaussian function

$$G(\omega') = \exp((-2\omega'/\Gamma_G)^2 \ln 2)$$

leading to the so called Voigt profile, which was approximated by a biquadratic form[38]

$$S(\omega) \sim (\Gamma_V/2)/[\alpha\omega^2 + (1 - \alpha)\omega^4/(\Gamma_V/2)^2 + (\Gamma_V/2)^2] \qquad (13)$$

Γ_G is the full line width at half-maximum of the Gaussian, Γ_V is the corresponding line width of the approximate Voigt profile, and α is a form factor. The latter varies between 0.5 for a pure Gaussian profile and 1 for a Lorentzian profile. The Mössbauer spectra below 200 K did not show relaxation effects and were reproduced as usual with a sum of Lorentzians for $\sigma(\omega)$ and with the source parameters $\Gamma_V = 0.17$ mm s^{-1} and $\alpha = 0.965$. These values were also used for the calculation of the relaxation spectra above 200 K. The parameters Γ_V and α are not independent. Meaningful values of Γ_V/Γ with the natural line width Γ of the corresponding Lorentzian can be obtained from a nomogram.[38] For $\sigma(\omega)$ the natural line width $\Gamma = 0.097$ mm s^{-1} was always inserted.

This procedure of evaluating Mössbauer relaxation spectra carefully accounts for the finite absorber thickness and calculates the convolution of the absorber and the source function. Most workers evaluate Mössbauer relaxation spectra using $\sigma(\omega)$ and introducing a combined source–absorber line width.[21,39] This is, even in the limit of thin absorbers, only valid for the Lorentzian contributions to $\sigma(\omega)$, as the convolution of two Lorentzians yields a Lorentzian with a composed line width. The convolution of the non-Lorentzian contributions to $\sigma(\omega)$ with the Lorentzian of the source, however, cannot be solved analytically. In addition, the composed line width is sometimes arbitrarily increased to account for line-broadening effects that do not arise from the relaxation process under study,[5] which certainly falsifies the Mössbauer time scale.

Table I. Mössbauer Parameters for $[Fe(2\text{-pic})_3](PF_6)_2$ Obtained from the Evaluation of the Spectra with the Two-State-Relaxation Model Described in the Text

T, K	$\Delta E_Q{}^H$, mm s^{-1}	δ_H,[b] mm s^{-1}	δ_L,[b] mm s^{-1}	$\gamma_H = t_{\text{eff}}{}^H/t_{\text{eff}}$	k_{HL}, 10^6 s^{-1}
80	2.55[a]	0.98[a]	0.420 (1)	0.032 (5)	
100	2.52 (2)	0.98 (1)	0.417 (1)	0.088 (5)	
110	2.531 (8)	0.964 (4)	0.415 (1)	0.129 (5)	
120	2.504 (11)	0.961 (6)	0.412 (1)	0.164 (5)	
130	2.483 (6)	0.953 (3)	0.408 (1)	0.210 (5)	
140	2.457 (6)	0.948 (3)	0.407 (1)	0.265 (5)	
150	2.438 (4)	0.940 (2)	0.400 (1)	0.329 (5)	
160	2.403 (4)	0.936 (2)	0.400 (1)	0.389 (5)	
170	2.364 (4)	0.929 (2)	0.394 (1)	0.448 (5)	
180	2.334 (4)	0.925 (2)	0.392 (2)	0.507 (5)	
190	2.293 (4)	0.918 (2)	0.390 (2)	0.564 (5)	
200	2.244 (4)	0.914 (2)	0.387 (2)	0.618 (5)	0.6 (2)
210	2.202 (4)	0.907 (2)	0.386 (3)	0.664 (6)	1.2 (2)
220	2.156 (4)	0.902 (2)	0.376 (4)	0.708 (6)	1.4 (2)
230	2.115 (5)	0.894 (2)	0.370 (7)	0.745 (6)	1.8 (2)
240	2.068 (5)	0.888 (2)	0.367 (10)	0.773 (6)	2.8 (2)
250	2.021 (6)	0.882 (3)	0.36 (2)	0.802 (6)	3.4 (3)
260	1.973 (7)	0.875 (2)	0.35[a]	0.834 (6)	4.2 (3)
270	1.921 (6)	0.862 (2)	0.35[a]	0.845 (6)	5.2 (4)
280	1.873 (10)	0.853 (4)	0.34[a]	0.860 (8)	6.0 (7)
285	1.850 (6)	0.85[a]	0.34[a]	0.882 (5)	6.4 (4)
290	1.825 (7)	0.85[a]	0.34[a]	0.888 (8)	6.6 (5)

[a] Parameter was not varied. [b] Isomer shifts are referred to ^{57}Co/Rh.

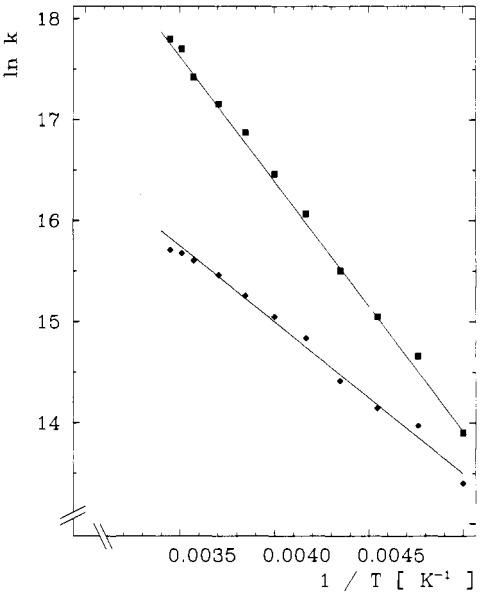

Figure 3. Arrhenius plot of the temperature dependence of the rate constants k_{HL} (◆) and k_{LH} (■) for $[Fe(2\text{-pic})_3](PF_6)_2$.

Results from the Relaxation Model and Comparison with Susceptibility Data. According to the theory described in the last two sections the spectra were fitted by six parameters: the effective thicknesses $t_{\text{eff}}{}^H$ and $t_{\text{eff}}{}^L$ of the HS and LS species, respectively, the isomer shifts δ_H and δ_L, the quadrupole splitting $\Delta E_Q{}^H$, and the relaxation rate k_{HL}. The rate k_{LH} of the reverse process was calculated from (5), where the HS fraction γ_H was taken as the ratio $t_{\text{eff}}{}^H/(t_{\text{eff}}{}^H + t_{\text{eff}}{}^L)$, assuming equal Debye–Waller factors for the HS and LS complex. Below 200 K, the Mössbauer spectra do not show relaxation effects and were fitted with $k_{HL} = 0$, above 200 K the rate k_{HL} was varied. Figure 2 shows that the line shapes of the spectra above 200 K are well reproduced by the described relaxation model. The remaining small deviations between experimental and theoretical spectra are presumably due to the texture of the crystalline material. The parameters obtained from the evaluation of the spectra are listed in Table I.

(37) Shenoy, G. K.; Friedt, J. M.; Maletta, H.; Ruby, S. L. *Mössbauer Eff. Methodol.* **1974**, *9*.
(38) (a) Meisel, W. *Exp. Tech. Phys.* **1971**, *19*, 23. (b) Müller, E. W. "MOSFUN", Mössbauer spectra fitting program for universal theories, user's guide, Mainz, FRG, 1980; available from: Steyens, J. G., Mössbauer Effect Data Center, University of North Carolina, Ashville, NC.
(39) Wickman, H. H.; Wertheim, G. K. In *Chemical Applications of Mössbauer Spectroscopy*; Goldanskii, V. I., Herber, R. H., Eds.; Academic: New York, London, 1968; p 548.

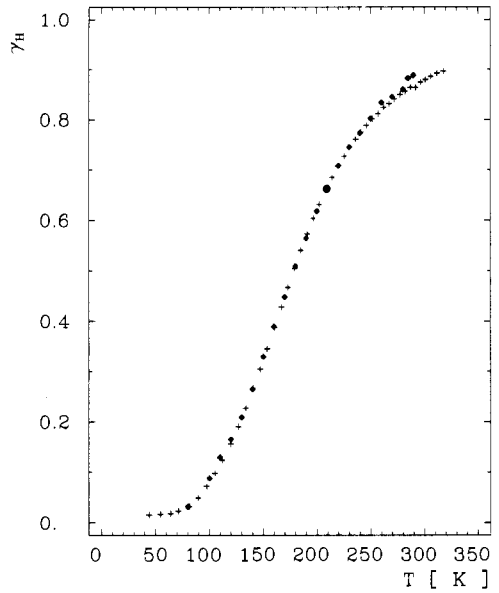

Figure 4. HS fractions γ_H derived from the susceptibility data (+) and from the evaluation of the Mössbauer spectra with a relaxation model (◆).

The plots of the ln k_{HL} and ln k_{LH} values vs the inverse of temperature (Figure 3) are essentially linear. Therefore, the kinetics of the spin conversion process can be described by an Arrhenius equation

$$k = \exp(-\Delta E/RT) \tag{14}$$

From the slope of a linear regression the activation energies are obtained as ΔE_{HL} = 12.5 (8) kJ mol^{-1} and ΔE_{LH} = 20.6 (6) kJ mol^{-1}. The corresponding intercepts are 20.9 (4) and 26.4 (3), respectively, yielding frequency factors $A_{HL} \approx 1 \times 10^9$ s^{-1} and $A_{LH} \approx 3 \times 10^{11}$ s^{-1}.

Finally, the HS fractions $\gamma_H = (1 - \gamma_L)$ derived from the Mössbauer spectra are compared with those from the susceptibility data. The susceptibility $\chi(T)$ is written as

$$\chi(T) = \gamma_H C_H/T + (1 - \gamma_H)\chi_L \tag{15}$$

For the susceptibility $\chi_H(T)$ of the paramagnetic HS complex a Curie law (Curie constant C_H) was assumed, and χ_L represents the temperature-independent susceptibility of the LS state. Unfortunately, the pure HS and LS phase of the present complex are not accessible. But assuming equal f factors for the HS and LS species the transition temperature $T_{1/2} = T(\gamma_H = 0.5)$ can be derived from the Mössbauer spectra. Inserting $T_{1/2}$ = 178.5 K (cf. Table I) and $\chi_L = 300 \times 10^6$ cm^3 mol^{-1} (the value for the similar complex $[Fe(2\text{-pic})_3]Cl_2$·EtOH) into (15), one obtains C_H = 3.38 cm^3/mol^{-1}/K. With these quantities $\gamma_H(T)$ was calculated from the measured susceptibilities for all other temperatures. Figure 4 shows a good agreement for the HS fractions derived from the effective thicknesses of the Mössbauer spectra and from the susceptibility data, even in the temperature range where the spin-state relaxation significantly alters the line shapes. This agreement justifies the assumption of equal f factors of the complexes in the HS and the LS states for the present compound.

Discussion

In the present study we have determined the ISC rates for an iron(II) spin-crossover complex in the solid state by a line shape analysis of the Mössbauer spectra. The ISC rates for the complex $[Fe(2\text{-pic})_3]^{2+}$ in solution, where a HS ⇌ LS equilibrium has been also found,[25] have not been determined yet. Nevertheless, it is interesting to compare our results with those obtained for other iron(II) complexes in solution. The ISC rates in solution around room temperature are within the range 4×10^5 s$^{-1} \leq k_{LH} \leq 1.7 \times 10^7$ s^{-1} and 5×10^6 s$^{-1} \leq k_{HL} \leq 2 \times 10^7$ s^{-1}, respectively.[8,11,13,14] For the present compound k_{HL} is within this range, whereas k_{LH} is larger. The spin conversion has been interpreted as a unimolecular reaction and the rate constants were written within absolute rate theory as[7,8]

$$k = \frac{k_B T}{h} \exp\left(-\frac{\Delta H^\ddagger}{RT}\right) \exp\left(\frac{\Delta S^\ddagger}{R}\right) \tag{16}$$

Here, $\Delta H^\ddagger$ represents the activation enthalpy and $\Delta S^\ddagger$ the activation entropy. In Table II these quantities are listed for $[Fe(2\text{-pic})_3](PF_6)_2$ together with the range of values that was derived from temperature-dependent data in solution.[8,11,13,14] It is noteworthy that the activation enthalpy $\Delta H_{HL}^\ddagger$, which is required to reach the activated complex from the HS state, is within the range of values found in solution. It can be concluded that the ISC rates in the solid state are not decreased by sizable lattice reorganization energies as has been suggested by Goldanskii[40] recently. Also, the activation entropy $\Delta S_{HL}^\ddagger$ is within the narrow range of values found in solution. Thus, the quintet–singlet conversion seems to be determined mainly by intramolecular factors. The activation enthalpy $\Delta H_{LH}^\ddagger$ for the reverse process in the present compound is smaller than the values found so far in solution. This is understood if one remembers that $\Delta H_{LH}^\ddagger$ contains the endothermic enthalpy contribution $\Delta H_{LH}°$, which arises from the difference of the potential energies of the HS and the LS state.

Table II. Activation Parameters for the $^1A_1 \rightleftharpoons {}^5T_2$ ISC in Iron(II) Spin-Crossover Complexes

complex	$\Delta H_{HL}^\ddagger$, kJ mol^{-1}	$\Delta H_{LH}^\ddagger$, kJ mol^{-1}	$\Delta S_{HL}^\ddagger$, J mol^{-1} K^{-1}	$\Delta S_{LH}^\ddagger$, J mol^{-1} K^{-1}
$[Fe(2\text{-pic})_3](PF_6)_2$	10.3 (8)	18.6 (6)	−78 (3)	−33 (3)
Fe(II) complexes in soln[8,11,13,14]	2.6–15.5	24–33	−58 to −95	−38 to −44
$[Fe_{0.1}Zn_{0.9}(ptz)_6](BF_4)_2$[38]	9.2		−145	

The value of $\Delta H_{LH}° \approx 8.3$ kJ mol^{-1} for the present compound is smaller than the values found in solution for several complexes, especially for the complex $[Fe(2\text{-pic})_3]^{2+}$, where a value of $\Delta H_{LH}° \approx 21$ kJ mol^{-1} has been estimated.[25] The smaller enthalpy $\Delta H_{LH}°$, which is required in the solid state to convert a LS to a HS complex, has been explained within the lattice expansion model developed in our group.[41] This model considers the elastic energy that is stored in the lattice containing small LS and larger HS complexes. If the HS complex fits better into the lattice than the LS complex, the conversion from LS to HS goes along with a decrease of the elastic energy of the lattice, so that the overall endothermic enthalpy change $\Delta H_{LH}°$, which is the sum of the intramolecular contribution and the lattice contribution, is decreased.[41] This also explains the lower transition temperature in the solid state as compared to the transition temperature in solution.

Further on, the present results can be compared with those obtained recently from a study of the relaxation kinetics of the light-induced metastable HS state in solid $[Fe_{0.1}Zn_{0.9}(ptz)_6](BF_4)_2$ (ptz = 1-propyltetrazole) at temperatures around 60–70 K (the activation parameters are listed in Table II).[42] The value for $\Delta H_{HL}^\ddagger$ is very similar, whereas $\Delta S_{HL}^\ddagger$ is considerably more negative for the trapped HS state in $[Fe_{0.1}Zn_{0.9}(ptz)_6](BF_4)_2$. A very large activation enthalpy (~30 kJ mol^{-1}) has been found by Ritter et al.[43] for the relaxation kinetics of nonequilibrium HS populations that were obtained by rapid cooling of solid $[Fe(paptH)_2](NO_3)_2$. This large $\Delta H_{HL}^\ddagger$ value is responsible for the observation of the nonequilibrium HS population even at temperatures above 100 K.

In conclusion, the ISC dynamics in solid $[Fe(2\text{-pic})_3](PF_6)_2$ do not show significant differences from the ISC dynamics of other

(40) Goldanskii, V. I. *Pure Appl. Chem.* **1983**, *55*, 11.
(41) (a) Spiering, H.; Meissner, E.; Köppen, H.; Müller, E. W.; Gütlich, P. *Chem. Phys.* **1982**, *68*, 65. (b) Adler, P.; Wiehl, L.; Meissner, E.; Köhler, C. P.; Spiering, H.; Gütlich, P. *J. Phys. Chem. Solids* **1987**, *48*, 517.
(42) (a) Hauser, A. *Chem. Phys. Lett.* **1986**, *124*, 543. (b) Hauser, A.; Gütlich, P.; Spiering, H. *Inorg. Chem.* **1986**, *25*, 4245.
(43) Ritter, G.; König, E.; Irler, W.; Goodwin, H. A. *J. Am. Chem. Soc.* **1978**, *17*, 225.

iron(II) complexes in solution. Therefore, the lattice influence on the dynamics of the HS ⇌ LS equilibrium seems to be less pronounced than the lattice influence on its thermodynamics. Line-broadening effects in the Mössbauer spectra are also observed for other iron(II) complexes.[44] We suppose that in these cases the dynamics of the spin equilibrium becomes detectable within the Mössbauer time scale.

Acknowledgment. We wish to express our thanks to Dr. H. Winkler, Lübeck, FRG, for helpful remarks concerning the evaluation of the Mössbauer relaxation spectra. Our sincere thanks are also extended to the Deutsche Forschungsgemeinschaft and the Fonds der Chemischen Industrie for financial support.

Registry No. $[Fe(2\text{-pic})_3](PF_6)_2$, 80105-98-2.

(44) (a) König, E.; Ritter, G.; Kulshreshta, S. K.; Nelson, S. M. *J. Am. Chem. Soc.* **1983**, *105*, 1924. (b) König, E.; Ritter, G.; Kulshreshta, S. K.; Waigel, J.; Sacconi, L. *Inorg. Chem.* **1984**, *23*, 1241.

Contribution from the University Chemical Laboratories, Cambridge, CB2 1EW England

Theoretical Study of Rearrangements in Boranes

David J. Wales* and Anthony J. Stone

Received March 9, 1987

In the following paper we present the results of a theoretical study of borane and carborane skeletal rearrangements. We show that tensor surface harmonic (TSH) theory is very useful in rationalizing the different energy barriers to rearrangement exhibited by *closo*-boranes and -carboranes. In particular, we are able to explain why the diamond–square–diamond (DSD) process is favored and to compare it with possible alternative mechanisms for $B_5H_5^{2-}$. We show that TSH theory provides a very simple selection rule for distinguishing symmetry-allowed from symmetry-forbidden processes: the latter involve transition states with a single atom on a rotation axis of order 3 or more. We combine this rule with the criterion that rearrangements involving smaller numbers of simultaneous DSD processes are most favorable to consider the relative energy barriers to skeletal rearrangement of the nido boranes and carboranes. Our conclusions are tested by approximate SCF calculation with the Fenske–Hall method, and some of the proposed transition states are investigated by ab initio SCF calculation with STO 4-31G basis sets and the CADPAC package to optimize geometries and evaluate force constants. The results suggest that for $B_8H_8^{2-}$ a single-DSD process leads to a transition state of distorted C_{2v} geometry. For $B_{12}H_{12}^{2-}$ the mechanisms previously proposed in the literature are found to be incorrect.

Introduction

Many years have passed since Alfred Stock synthesized the first boranes,[1] but the field of study that he opened up is still a fruitful one for both inorganic and theoretical chemists. Most theoretical effort has been directed toward an understanding of the electronic structure of boranes and carboranes in their experimentally observed equilibrium geometries,[2-9] and although recent work shows that this subject is by no means exhausted, they are reasonably well-understood. In contrast, the variation in magnitude of the energy barrier to skeletal rearrangements in these species is less well-understood—this is the problem we wish to address.

The diamond–square–diamond mechanism for the skeletal rearrangement of boranes was first proposed by Lipscomb.[10] In this process, illustrated in Figure 1, an edge common to two triangular faces of the cluster skeleton breaks and a new edge is formed perpendicular to it. DSD rearrangements, or combinations of several concerted DSD processes, have been proposed to rationalize fluxional processes and isomerizations of boranes, carboranes, and metallaboranes.[2,11] King[12] has used topological and group-theoretical considerations to distinguish between inherently rigid clusters (which contain no *degenerate* edges) and those for which one or more DSD processes are *geometrically* possible. An edge is said to be degenerate if a DSD rearrangement in which it is broken leads to a product having the same cluster skeleton as the starting material. For example, the three equatorial edges of $B_5H_5^{2-}$ are degenerate and the remainder are not. King's approach was partially successful in that all the structures he predicted to be rigid are found experimentally to be nonfluxional. However, some molecules of the $B_nH_n^{2-}$ series have geometrically allowed rearrangements involving one or more DSD processes but do not show any fluxional behavior.

Calculations at the PRDDO level have shown that $B_8H_8^{2-}$ and $B_{11}H_{11}^{2-}$ both have low-energy geometries corresponding to the postulated single-DSD-mechanism transition states.[13,14] Recently, Gimarc and Ott have used elementary group-theoretical arguments to show that the single-DSD processes which are geometrically allowed in $B_5H_5^{2-}$ and $B_9H_9^{2-}$ are both forbidden by symmetry (in the Woodward–Hoffmann sense) and that there is a symmetry-allowed double-DSD mechanism available for $B_9H_9^{2-}$.[15-17] These results highlight the need for a consistent theory to rationalize the experimentally observed order of fluxionality of *closo*-boranes and the directly related problem of the number of isolable carborane isomers in the $C_2B_{n-2}H_n^{2-}$ series of compounds. This is the subject of the following sections.

A graph-theoretical approach is appealing, owing to its simplicity and ease of interpretation. In particular, it might be

(1) Stock, A *Hydrides of Boron and Silicon*; Cornell University Press: Ithaca, NY, 1933.
(2) Wade, K. *Electron Deficient Compounds*; Nelson: London, 1971.
(3) Lipscomb, W. N. *Boron Hydrides*; Benjamin: New York, 1963.
(4) Wade, K. *J. Chem. Soc., Chem. Commun.* **1971**, 792.
(5) Wade, K. *Chem. Br.* **1975**, *11*, 177.
(6) Wade, K. *Adv. Inorg. Chem. Radiochem.* **1976**, *18*, 67.
(7) Rudolph, R. W.; Pretzer, W. R. *Inorg. Chem.* **1972**, *11*, 1974.
(8) Rudolph, R. W. *Acc. Chem. Res.* **1976**, *9*, 446.
(9) Williams, R. E. *Adv. Inorg. Chem. Radiochem.* **1976**, *18*, 67.
(10) Lipscomb, W. N. *Science (Washington, D.C.)* **1966**, *153*, 373.
(11) See e.g.: Kennedy, J. D. In *Progress in Inorganic Chemistry*; Wiley: New York, 1986; Vol. 34.
(12) King, R. B. *Inorg. Chim. Acta* **1981**, *49*, 237.
(13) Kleier, D. A.; Lipscomb, W. N. *Inorg. Chem.* **1979**, *18*, 1312.
(14) Kleier, D. A.; Dixon, D. A.; Lipscomb, W. N. *Inorg. Chem.* **1978**, *17*, 166.
(15) Gimarc, B. M.; Ott, J. J. *Inorg. Chem.* **1986**, *25*, 83.
(16) Gimarc, B. M.; Ott, J. J. *Inorg. Chem.* **1986**, *25*, 2708.
(17) Gimarc, B. M.; Ott, J. J. *J. Comput. Chem.* **1986**, *7*, 673.

0020-1669/87/1326-3845$01.50/0